Journal of Applied Sciences

ISSN 1812-5654

science alert

ANSInet
an open access publisher
http://ansinet.com

Journal of Applied Sciences 11 (16): 3022-3027, 2011
ISSN 1812-5654 / DOI: 10.3923/jas.2011.3022.3027

Investigation of Humidity Effect on the Air Refractive Index using an Optical Fiber Design

[1]A. Mehrabani and [2]H. Golnabi
[1]Department of Physics, Tehran North Branch, Islamic Azad University, Iran
[2]Institute of Water and Energy, Sharif University of Technology, Tehran, Iran

Abstract: In this study operation of an optical design based on the intensity modulation for the refractive index change has been described. The reported instrument measures the transmitted output power depending up on the medium refractive index in the light path of a fiber-to-fiber design. A liquid cell is located between the fibers in the light path and power variations for different cold and hot water levels in the cell are measured. By using a reference humidity meter the calibration curve representing the relative humidity (%RH) as a function of the transmitted output power is obtained. For the hot water with the final temperature of T = 32.7°C the output power range of 255.0 -313.0 nW is measured for a relative humidity change of 32.76 -41.26%. A power variation of 58 nW is noted for the 8.5% RH variation which shows the high sensitivity for the reported sensor. For the light transmitted in dry air path the output power is 516.7 nW while for the water path such power is 784.6 nW. Thus, the reported device can check the presence of the water vapor, water, or any other transparent liquid in the gap between the two axially aligned fibers. Performance of the new system is satisfactory as a refractive index monitoring mean and for the water/water vapor sensing.

Key words: Light detection, water vapor, sensor, intensity modulation

INTRODUCTION

Light guides are transparent devices that conduct the flow of light from a source to the point of interest and optical fibers are one of the most effective links in this respect. An optical fiber has a transparent inner core and a thin exterior cladding and a protective buffer jacket. A silica Glass Optical Fiber (GOF) has a better light transmission characteristic with the less loss in comparison with the Plastic Optical Fiber (POF) and can tolerate higher temperatures than plastic fibers. Fiber material absorption is related to the material composition, refractive index and the fabrication process of the fiber (Senior, 1992). Fiber attenuation is a strong function of the light wavelength, depends on the temperature and aging of the transmitting fiber. The plastic optical fibers can operate successfully at visible wavelength range (650 nm) with a typical white light attenuation of 0.2 to 0.25 dB km^{-1} (Grattan and Sun, 2000).

Plastic optical fibers are used in the optical systems and scanners for the short distance light transmission and can be also used for the sensing operations (Grattan and Sun, 2000). Such fiber sensors can be designed based on the certain losses at the interfaces in the fiber-to-fiber arrangement. Different reports on the design, characterization, operation and possible applications of optical fiber sensors have been given in literature (Zhang *et al*., 2007; Grattan and Sun, 2000; Haus, 2010; Golnabi *et al*., 2007). In many optical systems optical fibers are used to transmit the source light for power delivery or image processing (Asadpour and Golnabi, 2008; Jafari and Golnabi, 2008; Haghighatzadeh *et al*., 2009; Asadpour and Golnabi, 2010). Physical and chemical effects have been used to develop a variety of optical probe systems for monitoring different parameters (Wade *et al*., 2000; Yin *et al*., 2008). Plastic Optical Fiber (POF) offers some advantages such as component cost, ease of handling and connections, flexibility, visible wavelength operating range, high numerical aperture (0.5), low cost test equipment and low overall system cost (Golnabi and Azimi, 2007, 2008; Jafari and Golnabi, 2010). Such advantages over Glass Optical Fiber (GOF) make them attractive for a number of applications including sensor designs. In the reported experiments similar POFs are utilized and based on the light intensity modulation a variety of sensors are designed.

On the other hand, a variety of experimental and theoretical investigations have been made to study the air humidity effects on the performance of the optical systems at sea level with a high amount of water vapor (Levi, 1980). With new advances in the field of optical fibers and using the fiber-to-fiber design the goal is to study the important role of the humidity on the air refractive index variation. The objective of this study is to

Corresponding Author: Hossein Golnabi, Institute of Water and Energy, Sharif University of Technology, Tehran, Iran
Tel: +98 21 66164126 Fax: +98 21 66005118

demonstrate that the reported optical design can be implemented to check the presence of the water vapor/water in the fiber gap. It is also our goal to show that such an optical design can be used for the construction of a humidity sensor. Experimental results and theoretical descriptions concerning the performance of such sensors are reported here.

MATERIALS AND METHODS

Development of the reported method and the experimental work are performed for the period of 2010-2011 in the Institute of Water and Energy of the Sharif University of Technology. Consider two aligned axial fibers with the air gap that provides two fiber core-air and air-core interfaces as shown in Fig. 1. If a beam of light with the transmission factor of T_1 in the first fiber is incident on the first core-air interface at an angle θ_1, the reflected part is shown by R_1 and the rest is transmitted into the air gap. A limited cone of this light is then reflected from the air-core interface of the second fiber with amplitude R_2 before finally transmitted into the second fiber at air-core interface. Using Fresnel relations for R and absorption/scattering law for A, the expression for transmission of the light emerging at the second air-core interface for the polarized and unpolarized light can be obtained. With some approximations (ignoring axial misalignment loss, index mismatching, etc.) the light transmission factor in the second fiber is:

$$T_{air} = T_1 - R_1(\theta_1, n_c, n_a) - R_2(\theta_1, n_c, n_a) - A(n_a, \alpha_a, d) + C(\theta_1, n_c, n_a) \quad (1)$$

where, n_c is the refractive index of the fiber core, d is the optical path in the gap medium, α-absorption factor and C is the light coupling factor. For air this coupling factor due to beam divergence is relatively large. For the presence of a water liquid in the gap (Fig. 1), the water liquid forms a wave guide transmission line instead of the regular light propagation in the air gap. Transmission factor for this case is given by:

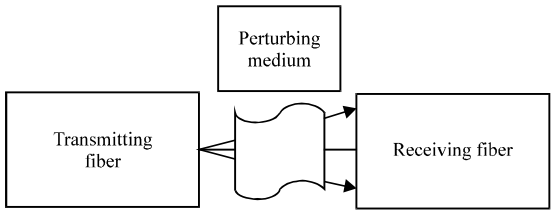

Fig. 1: Block diagram for the fiber-to-fiber arrangement and light medium perturbation

$$T_{liq} = T_1 - R_1(\theta_1, n_c, n_{liq}) - R_2(\theta_1, n_c, n_{liq}) - A(n_{liq}, \alpha_{liq}, d) + C(\theta_1, n_c, n_{liq}) \quad (2)$$

where, n_{liq} is the index of refraction for the filling water liquid. In this case the coupling factor C is higher than that of air gap case because of an additional wave guide is formed. This optical waveguide provides required condition for the Total Internal Reflection (TIR). Since R_1 and R_2 is usually less for the case of water liquid filling and coupling factor C is larger, thus the transmitted light into the second fiber is increased in the presence of water liquid.

On the other hand for the case that absorption and scattering loss (A) is the dominant factor rather than C, then the emerged intensity of the light into the second fiber is less for the case of liquid path instead of the light air path. As a result, a decrease in the transmitted light is obtained for the modulated intensity. The output signal of the sensor defined by T_{liq} and power modulation depends upon any change in the refractive index n_{liq}. The transmitted power is the highest in the case that the TIR condition is satisfied in the generated wave guide. Then even a small change in the Refractive Index (RI) of the filling medium leads to a large modulation in the intensity of transmitted light.

For the case of humid air the relation (1) is replaced by:

$$T_{hum-air} = T_1 - R_1(\theta_1, n_c, n_{ha}) - R_2(\theta_1, n_c, n_{ha}) - A(n_{ha}, \alpha_{ha}, d) + C(\theta_1, n_c, n_{ha}) \quad (3)$$

where, $T_{hum-air}$ shows the transmitted power to the second fiber for the case of the humid air between the two fibers and n_{ha} is the refractive index for the humid air containing water vapor. As can be seen monitoring of the n_{ha} is possible by measuring the variation of the transmitted light power.

Figure 2 shows the experimental arrangement of the designed system. It consists of a light source, a liquid cell,

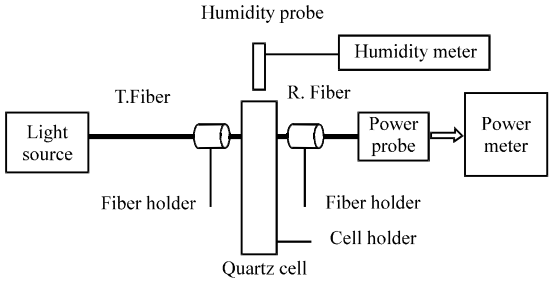

Fig. 2: Experimental arrangement of the power measurements

transmitter and receiver fibers, mechanical holders for the fibers and the cell, humidity probe and meter, light power probe and a light power meter. For the light illumination in this design it is possible to use a diode laser, a He-Ne laser, white lamp, or a LED as the light source. To test the constructed device a white lamp is used for the described measurements. In our system the supply voltage for the lamp is 15 V DC and lamp operates at visible wavelength orange with the nominal wavelength of 550 nm. The power supply provides the required regulated voltages (10-20 V). A digital power meter (SANWA, OPM-37) is used for the transmitted power reading and data acquisition.

Our design uses a long transmitter plastic fiber (40 cm) and a short receiver optical fiber (4 cm) in the fiber-to-fiber arrangement. The overall diameter of the multimode fiber is 2.2 mm; the cladding diameter of about 1 mm and the core diameter of 0.860 mm. Plastic optical fiber can operate successfully at wavelengths from 450 to 1300 nm. Since plastic optical fibers have larger diameters (about 1 mm) than glass fibers (8-100 microns), their connectors are less complex, cost less and are less likely to suffer damage than connectors for glass fibers. In this design as shown in Fig. 2, the source light emerged from the transmitter fiber is transmitted through the liquid cell and collected by means of the receiver fiber that is connected to the power meter probe photodetector. The output signal is monitored by adding the water liquid to the cell and dry wet signals are measured accordingly. A quartz cell with 10×10 mm cross section and 40 mm long is used in this design as liquid container and the cell wall thickness is about 0.5 mm which offers low transmission losses with an effective path length of 9 mm.

In order to calibrate the system a humidity meter (YK-80HT) is used in this experiment. It includes a humidity and temperature probe head which shows the relative humidity and temperature separately on the LCD display meter. The unit provides options for reading the dew point as well. The instrument offers a 0.01% RH resolution for the humidity and 0.01°C resolution for the temperature. It has a fast humidity measuring response time with high accuracy and precision in measurements. Humidity measuring range for the described device is 10 to 95% RH. The accuracy of the device for the humidity range greater than 70% RH is about (3 reading + 1% RH) and for the range smaller than 70% RH is about (3% RH and for temperature range of 0-50°C is about 0.8°C. To generate humidity in this set up usually cold and hot water samples are used to generate the humidity to a certain level.

Experimental results: In given analysis when the light path in the flow cell is in liquid the output signal referred to as the wet signal and when the light path is air it is called the dry signal. For the case that there is a minor water vapor in the air it is referred to as the humid air signal. For the case of dry signal the nominal refractive index of the transmitting air is one while for the water liquid case is equal to 1.33 and for the humid air is generally in the 1-1.33 range. As a result the amount of the light coupling as described in the theoretical part depends on this index of the refraction of the transmitting medium. Such light intensity modulation has been used for the humidity sensing using the designed device. The output signal depends on two factors namely the loss factor and the light convergence factor as described.

Figure 3 shows the dry, humid air signal and wet output power signals for the air refractive index of about 1 and for the water liquid with the index of refraction of about 1.33. To change the percentage of the humidity of the cell and as a result the fiber gap the amount of the water is increased gradually and output power is recorded, accordingly. In practice before adding water to the cell the dry signal is measured at least five times and the average value is shown. For the case of adding water the signal measurement is performed five times and averaged values are shown. At dry condition the output power for dry air is about 516.7 nW. for 1 cc water the output power is 546.6 nW, For 2 cc the power is 744.0 nW, for 3 cc is about 774.2 nW. The total volume of the operating cell is about 4 cc and for this volume of water the entire beam path length is filled with the water and for this case the wet signal power is about 784.6 nW. As can be seen by increasing the water in the cell the humidity is increased and as a result one can see that the refractive index for the dry air is the minimum amount while for the case of adding water the humidity is increased and as a result the humidity has increased the refractive index of the air in the fiber to fiber path length. On the other hand when the gap is filled with the water liquid the output power is the maximum value of about 784.6 nW.

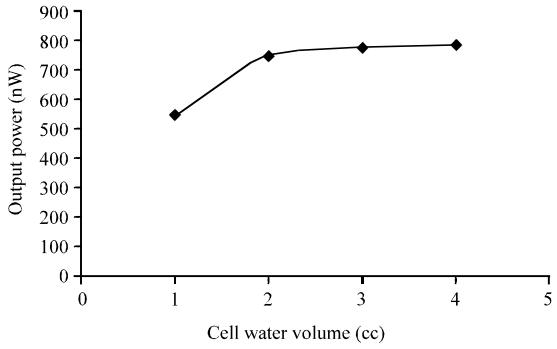

Fig. 3: Output power variation as a function of the cell liquid volume

Figure 4 shows the same experiment for the cold (T = 21°C) and hot water (final temperature of T = 32.7°C). The dry and wet output power signals for water liquids at different temperature are compared in this experiment. The output powers are compared for the early stage of adding water to the cell for about 0-4 sec. As can be seen, the behaviors for the cold and hot water samples are different. The power variation for the cold water addition case is similar to the case shown in Fig. 3 but for the hot water a peculiar power variation occurs. In this case for 1 cc hot water the output power is 495.4 nW, For 2 cc the output power is increased to 927.0 nW, for 3 cc the power is decreased to about 685.0 nW. As mentioned the total volume of the operating cell is about 4 cc and for this volume of water the entire beam path length is filled with the water and for this case the wet signal power in this case is increased to about 798.0 nW. By comparing the result with that of cold water it is noted that the drop of output power at 3 cc is because of the decrease in the water vapor generation at this time. Such drop in the amount of the air humidity has caused the reduction in the transmitted light power.

Comparison of the output power variation for the hot water at different times is investigated in this section. Output variations as a function of the cell water volume for the hot water sample for the short time (3 sec) and long time of (30 sec) are investigated. Figure 5 shows the experimental results for the hot water (final temperature of T = 32.7°C). The dry and wet output power signals for water liquid at different times are compared in this experiment. The output powers are compared for the early stage of adding water to the cell for about 3 sec and also for the time passage of about 30 sec. As can be seen, the behaviors for the water sample as a function of time are different. The power variation for the hot water addition case is similar to the case of cold water as shown in Fig. 3 but for the hot water at long time a peculiar power variation occurs. In this case for 1 cc hot water the output power is 628.0 nW, For 2 cc the output power is increased to 670.0 nW, for 3 cc the power is decreased to about 661.0 nW. As mentioned the total volume of the operating cell is about 4 cc and for this volume of water the entire beam path length is filled with the water and for this case the wet signal power in this case is increased to about 718.0 nW. By comparing the of the hot water samples it is noted that the drop of output power at 3 cc is because of the decrease in the water vapor generation at this time. Such drop in the amount of the air humidity has caused the reduction in the transmitted light power.

Humidity variation as a function of the output power variation for the reported probe is studied in the last section. In order to calibrate the measuring system in Fig. 6 the relative humidity (%RH) is plotted as a function of the transmitted output power for the hot water with the final temperature of T = 32.7°C. For the output power of 255.0 nW, the relative humidity is 32.76%, for 266.5 nW is

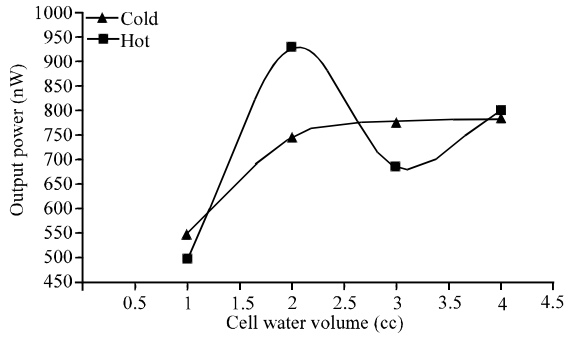

Fig. 4: Output variation as a function of the cell water volume for the long time

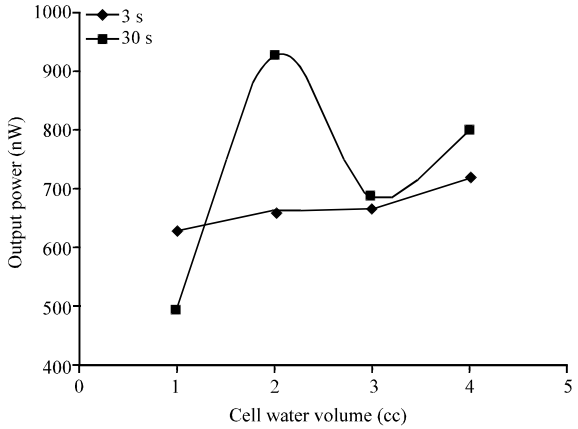

Fig. 5: Comparison of output power variations for the hot water as a function of time for hot water samples

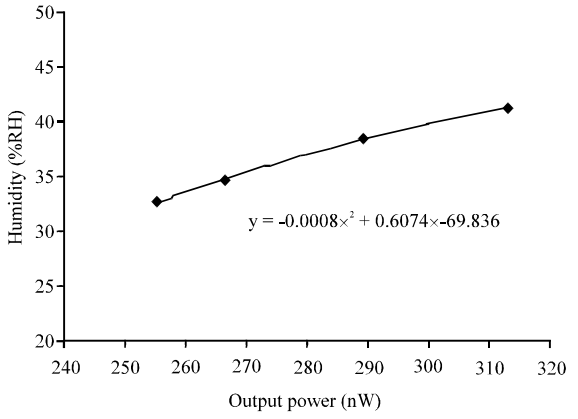

Fig. 6: Humidity variation as a function of the output power change for the reported cell probe

34.4, for 289.5 nW is 38.55% and finally for the 313.0 nW power the relative humidity is 41.26%. The experimental measurements are shown with the diamond shape data points while the trend line option of the Excel program is used to obtain the governing equation and the calibration curve. As can be seen in Fig. 6, the calibration curve shown here is for the power range of 255 to 315 nW corresponding for the RH range of 30-42%. However, such an extrapolated equation can also be obtained and used for the lower and higher humidity ranges.

DISCUSSION

Fundamentals of the optical fiber communications and optical loss mechanism in optical fibers are described extensively (Crisp and Elliott, 2005). To explain the experimental results consider the Factor C in Eq. 1 which is related to the dry air and the C factor depends on the Numerical Aperture (A). For the water path length Eq. 2 gives a higher Coupling factor C and from Eq. 3 for the humid air the C factor is somewhere between that of dry air and wet water. To explain the coupling factor consider the numerical Aperture (A) for the three cases. For the dry air (Fig. 1) we have:

$$A_0 = n_a \sin\alpha_a \quad (4)$$

where, alpha is the incident angle on the second receiving fiber. With some approximations the value of this angle is similar for the mentioned gap mediums. For the case of humid air one can write:

$$A_{ha} = n_{ha} \sin\alpha_{ha} \quad (5)$$

whereas, the numerical aperture in this case is increased because the refractive index n_{ha} is higher that n_a given in Eq. 1. Similarly for the water medium the numerical aperture is given by:

$$A_{liq} = n_{liq} \sin\alpha_{liq} \quad (6)$$

where, n_{liq} is for water that is about 1.33 and as a result by increasing the medium refractive index for given cases the collecting power by the second fiber has been increased and as a result the transmitted power is increased, accordingly.

Assuming the sinus value to be nearly similar for three cases, then numerical apertures are mainly depends on the refractive index of the medium. As a result of the bigger aperture, A, for the receiving fiber the transmitted power is higher for the higher numerical aperture values. The refractive index measurements of the air by interferometry are given in literature (Mc Murtry *et al*., 2001). In another study refractive index of air and related equations for the visible and near infrared region of the spectrum are reported (Ciddor, 1996). Some considerations about the atmospheric optics and the role of air humidity on the refractive index are also described in the literature (Levi, 1980).

A humidity sensor based on a hetero-core optical fiber is reported recently (Akita *et al*., 2010). In the given design the refractive index of the polymer layer coated on the hetero-core region varies with the relative humidity around the sensor. Therefore, the transmitted light in the fiber is affected by such an index variation. They measured an intensity change of 0.26 dB at a wavelength of 1310 nm in the range of 50-92.9% RH. In another study a high-speed humidity sensor is reported that is fabricated from a nanostructured titanium dioxide thin film (Steele *et al*., 2006). A gradient index optical filter is designed by glancing angle deposition acting as a sensor. Under varying humidity condition the transmittance spectrum of the interference filter shifts due to effective refractive index change of the porous structure resulting from water vapor adsorption. Using such a sensor the light transmittance for 650 nm wavelength at various humidity levels (5-90% RH) is measured with a high-speed sensing (adsorption time of 270 ms). In that design a transmittance change of 30% is reported for the 85% RH change.

In the experiment reported here the modulated transmitted light powers at wavelength of 500 nm are measured. For the output power of 255.0 nW, the relative humidity is 32.76% and for the 313.0 nW power the relative humidity is 41.26%. As can be seen here a power variation of 58 nW is noted for the 8.5% RH variation which shows a compatible sensitivity for the reported sensor. Considering our results there is a general agreement between the measured results and those described by other investigations with a compatible performance. However, the reported sensing design is more simple and cost effective. Also there is a good correlation between the theoretical modeling given for the air refractive index variation and the measured modulated output powers.

CONCLUSION

The effects of the humidity on the air refractive index were investigated by the fiber-to-fiber optical method. Useful information for different situations is given here and it is shown that intensity modulation can be used to study the refractive index variation in a precise way. Obtained results show that light modulated power signals

can provide information about the refractive index media filling the gap between the two transmitting fibers. By experimenting different filling air conditions it is noticed that the modulated power signal depends on both the axial separation of the fibers as well as the refractive index of the gap medium. Using this technique one can extract information concerning the optical properties of fiber-to-fiber filling gap and as a result the refractive index variation with the humidity. In this way presence of small percentage of the humidity in the gap medium can be detected with a high sensitivity. As a major conclusion the reported device can check by measuring the modulated power and the presence of the water vapor, water, or any other transparent liquid in the gap between the two axially aligned fibers.

ACKNOWLEDGMENT

This work was supported in part by the Sharif University of Technology Research programme. The authors gratefully acknowledge the grant money devoted to this research project (Grant No. 3104).

REFERENCES

Akita, S., H. Sasaki, K. Watanabe and A. Seki, 2010. A humidity sensor based on a hetero-core optical fiber. Sens. Actuators B: Chem., 147: 385-391.

Asadpour, A. and H. Golnabi, 2008. Beam profile and image transfer study in multimode optical fiber coupling. J. Applied Sci., 8: 4210-4214.

Asadpour, A. and H. Golnabi, 2010. Fiber output beam shape study using imaging technique. J. Applied Sci., 10: 312-318.

Ciddor, P.E., 1996. Refractive index of air: New equations for the visible and near infrared. Applied Opt., 35: 1566-1573.

Crisp, J. and B.J. Elliott, 2005. Introduction to Fiber Optics. 3rd Edn., Elsevier, New York, ISBN-13: 9780750667562.

Golnabi, H. and P. Azimi, 2007. Design and performance of a plastic optical fiber leakage sensor. Opt. Laser Technol., 39: 1346-1350.

Golnabi, H., M. Bahar, M. Razani, M. Abrishami and A. Asadpour, 2007. Design and operation of an evanescent optical fiber sensor. Opt. Lasers Eng., 45: 12-18.

Golnabi, H. and P. Azimi, 2008. Design and operation of a double-fiber displacement sensor. Opt. Commun., 281: 614-620.

Grattan, K.T.V. and T. Sun, 2000. Fiber optic sensor technology: An overview Sensors Actuators A, 82: 40-61.

Haghighatzadeh, A., H. Golnabi and M. Shakouri, 2009. Design and operation of a simple beam shaping system. J. Applied Sci., 9: 3350-3356.

Haus, J., 2010. Optical Sensors, Basics and Applications. Wiley-VCH, New York, ISBN-13: 978-3527408603, pp: 189.

Jafari, R. and H. Golnabi, 2008. Spectral analysis using a new opto-mechanical instrument. J. Applied Sci., 8: 3669-3675.

Jafari, R. and H. Golnabi, 2010. Simulation of three different double-fiber probes for reflection sensing. J. Applied Sci., 10: 20-28.

Levi, L., 1980. Applied Optics: A Guide to Optical System Design. Vol. 2. John Wiley and Sons, New York.

Mc Murtry, S., J.D. Wright and D.A. Jackson, 2001. Sensing applications of a low-coherence fiber optic interferometer measuring the refractive index of air. Sens. Actuators B: Chem., 72: 69-74.

Senior, J.M., 1992. Optical Fiber Communications: Principles and Practice. 2nd Edn., Prenticle Hall, New York, USA., ISBN-13: 9780136354260, pp: 922.

Steele, J.J., A.C. van Popta, M.M. Hawkeye, J.C. Sit and M.J. Brett, 2006. Nanostructured gradient index optical filter for high-speed humidity sensing. Sen. Actuators B: Chem., 120: 213-219.

Wade, S.A., G.W. Baxter, S.F. Collins, K.T.V. Grattan and T. Sun, 2000. Simultaneous strain-temperature measurement using fluorescence from Yb-doped silica fiber. Rev. Sci. Instrum., 71: 2267-2269.

Yin, S., P.B. Ruffin and F.T.S. Yu, 2008. Fiber Optics Sensors. 2nd Edn., CRC Press, Taylor and Francis Group, New York, ISBN-13: 9781420053654, pp: 477.

Zhang, X., W. Bai and Y. Chen, 2007. An approach for accurate measurement of lubricant film thickness based on fiber-optical displacement sensor. Proceedings of the International Conference on Mechatronics and Automation, Aug. 5-8, Harbin, pp: 3015-3019.